DeltaBot construction for presentation and study of kinematics

Adam Hrežo
Department of Microelectronics
Brno University of Technology
Brno, Czech Republic
247008@vutbr.cz

***Abstract*— This article focuses on the potential use of rotary delta-type structures for 3D printing. It also analyzes the DeltaBot construction and describes and designs its main structural components.**

Keywords—FDM, 3D printer, Rotary Delta, kinematics, Klipper, firmware

I. INTRODUCTION

DeltaBot or Rotary Delta robots are often used in industry due to their speed and relatively good accuracy. They are designed for the rapid transfer of small, lightweight parts. This work focuses on the design of the main structural components. It also covers the assembly and commissioning of the proposed printer.

The goal of this project is to design and build a fully functional DeltaBot-type FDM 3D printer for public demonstrations and kinematics research.

II. ROTARY DELTA ROBOTS

Rotary delta printers are a recent innovation and are not yet available on the market. Due to this fact, only a limited amount of information can be found about them.

This chapter therefore focuses mainly on the construction and principle of rotary delta robots, as these robots are commonly used in industry, with the only difference being the type of end effector— in the case of a 3D printer, the hotend. A rotary delta robot is a parallel-type robot with three degrees of freedom.

A. Structural Components of the DeltaBot

Rotary delta robots consist of several key structural components. The base is the part of the robot where arm actuators are mounted. The arms (driving arms) transmit the rotational motion from the actuators to the struts (following arms), which are connected to the arms through joints. Finally, the end platform is attached to the struts via joints [1][2].

B. Principle of the Rotary Delta robot

Now that the main structural components of this type of robot are known, it is possible to describe how this printer works. The rotary delta has an interesting kinematic system. The position of the end platform is determined by the position (rotation) of the three arms.

From the perspective of inverse kinematics, the process works as follows. First, the absolute coordinates of point *V*, which represents the position of the end effector as specified in G-code, are converted into relative coordinates *M1* (1),(2), *M2* (3),(4), and *M3* (5),(6) for each of the three arms individually. This calculation determines the relative coordinates of the connection points between the struts and the end platform (Fig. 1) [3][4].

$$X_{M1} = X_V + d\cos(\alpha_1) = X_V + d \cdot \cos(90) = X_V \quad (1)$$
$$Y_{M1} = Y_V + d\sin(\alpha_1) = Y_V + d \cdot \sin(90) = Y_V + d \quad (2)$$

$$X_{M2} = X_V + d\cos(\alpha_2) = X_V - d \cdot \cos(210) \quad (3)$$
$$Y_{M2} = Y_V + d\sin(\alpha_2) = Y_V - d \cdot \sin(210) \quad (4)$$

$$X_{M3} = X_V + d \cdot \cos(\alpha_3) = X_V + d \cdot \cos(330) \quad (5)$$
$$Y_{M3} = Y_V + d \cdot \sin(\alpha_3) = Y_V - d \cdot \sin(330) \quad (6)$$

where *d* is the radius of an imaginary circle centered at point V, passing through all three points $M1$, $M2$ and $M3$.

The following is the transformation of the coordinates M_1, M_2 *and* M_3 ,which are located in the main coordinate system, into the coordinates M_1', M_2' *a* M_3', where each of these points is located in its own coordinate system (7),(8).

$$X' = M_Y \sin(\beta) + M_X \cos(\beta) \quad (7)$$
$$Y' = M_Y \cos(\beta) - M_X \sin(\beta) \quad (8)$$

where β is the angle between the positive direction of the Y-axis and each of the M points. In this case: $\beta_1 = 0°, \beta_2 = 120°, \beta_3 = 240°$ (Fig. 1).

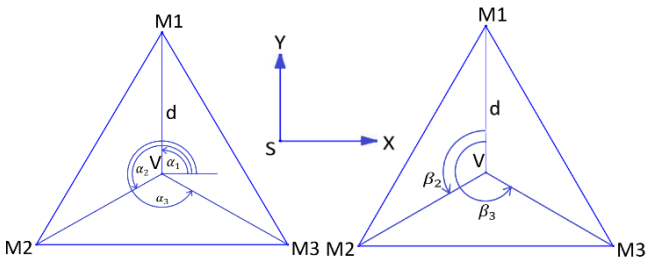

Fig. 1. Graphical representation of key points of the end platform for kinematics calculation.

Next, for each arm, the intersection P is found between a circle formed by the arm k, centered at point Q, and a sphere formed by the strut l, centered at point M (9),(10).

$$(X' - X'_M)^2 + (Y' - Y'_M)^2 + (Z - Z_M)^2 = l^2 \quad (9)$$

$$\left(X' - X'_Q\right)^2 + \left(Z - Z_Q\right)^2 = k^2 \quad (10)$$

where X'_M, Y'_M and Z_M are the coordinates of the strut attachment point of length l on the end platform. X'_Q and Z_Q are the coordinates of the arm rotation point of length k (Fig. 2).

After simplifying and solving these two equations, there is a simple formula for calculating the angle theta:

$$\theta = arctan\left(\frac{Z_Q - Z_P}{X'_P - X'_Q}\right) \quad (11)$$

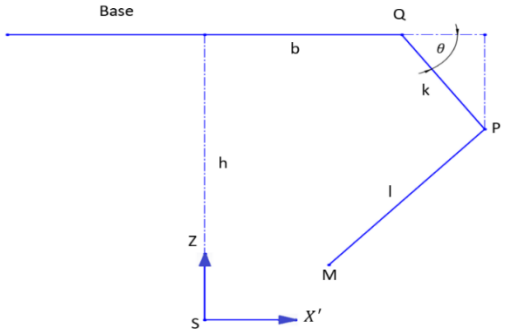

Fig. 2. 2D representation of the connection between the strut of length l and the end platform at point M, and the arm of length k, which is connected to the base at point Q.

III. DESIGN OF STRUCTURAL COMPONENTS OF THE DELTABOT PRINTER

A. Printer Frame

The first step in designing the structural components of the printer frame is determining the required print volume. The size of the working area depends on the maximum achievable height of the printing space. When choosing a cylindrical working volume, it is important to consider that the larger the selected print surface, the smaller the attainable print height. For this printer, a round heated bed on an aluminum substrate with a diameter of 220 mm was selected, with a maximum print height of approximately 150 mm.

Based on this information, the frame's connecting components were designed. The proposed construction of this printer differs from a typical rotary delta (DeltaBot) configuration in that the base is positioned at the bottom near the ground. Consequently, the print bed is located at the top. This arrangement could have several potential advantages. For example, since the actuators for the individual arms, which add weight, are located on the base, the center of gravity of the printer shifts downward. This should have a positive impact on vibration resistance, leading to improved print quality. Additionally, the control electronics would be positioned below the base.

B. Arm Actuation

In DeltaBot actuators, when using standard NEMA17 stepper motors, these motors alone do not provide sufficient torque to move the arms, which support the entire weight of the print head, including the struts, joint connections, and structural components. One option is to use larger and therefore more powerful motors. However, larger motors are more expensive and require higher power consumption. Another alternative is to use mechanical transmission to increase the torque of the actuator.

After consideration, a 5:1 belt drive was chosen, consisting of a NEMA17 stepper motor, a GT2 belt (10 mm wide, 200 mm long), and two pulleys with 16 and 80 teeth. This gear ratio should be sufficient given the structural parameters. The drive is mounted to the printer's base using two PLA-printed brackets.

C. Joints

One of the key structural components of a rotary delta printer is the joint connections, which movably link the end platform to the struts and the struts to the arms. These joints must meet several requirements, such as low weight, minimal backlash, long lifespan, and a large angular range [5]. The larger the angular range of the joint, the greater the working space of the device, in this case, the printer. In DeltaBot-type constructions, ball joints with three degrees of freedom are commonly used. Standard ball joints typically allow an angular range of approximately ±15° to ±18°.

For this printer, commonly available stainless steel spherical joints were used due to their simplicity and low cost. These joints were mounted in 3D-printed holders made from copolyester filament with 20% of carbon fiber, ensuring both strength and low weight (about 25 g) of the entire joint assembly (Fig. 3).

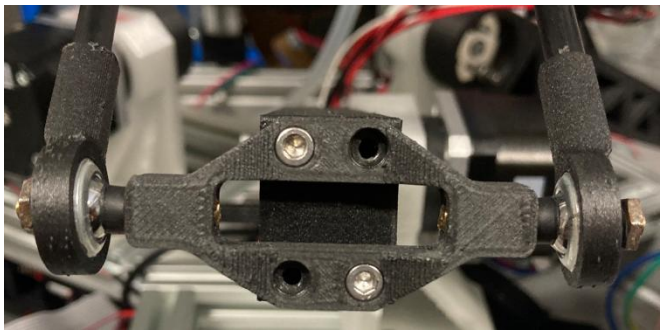

Fig. 3. Assembly consisting of two spherical joints linked by a connector.

D. Arms and Struts

To achieve the highest possible printing speed, all components of the moving parts must be as lightweight as possible. This applies to both the arms and the struts.

For this reason, a second arm was designed using a composite material. The arm is 3D printed from PA-CF, making it very strong while remaining relatively lightweight. A metal flange coupling was used to attach the arm to its actuator (the output shaft of the gearbox) (Fig. 4). The assembled arm weighs approximately 42 g. The total length of the arm, including the joint connector, is 151.8 mm.

Fig. 4. 3D printed arms.

The struts were designed as carbon fiber tubes with an inner diameter of 4 mm, an outer diameter of 6 mm, and a length of 245 mm. These carbon tubes proved to be an excellent solution, as they provide sufficient strength while keeping the minimal weigh. The total length of a strut including both spherical joints is 300 mm.

E. End platform

Just like the arms, struts, and joints, the end platform is a crucial component of this printer.

It houses several essential parts: a 3010 fan for active cooling of the coldend heatsink, a Bowden extruder, an inductive sensor for print bed calibration, and an aluminum tube that directs airflow to cool the deposited material (Fig. 5). Additionally, the platform contains joint components for connecting the struts to the platform.

As one can see, the platform holds multiple components, and at high accelerations, their weight could cause flexing. To prevent this, the final version of the platform was made from a carbon fiber composite plate, similar to the arms. First, the platform's outline and the extruder mounting hole were cut using a water jet cutter. However, the used water jet was unable to cut holes smaller than 5 mm in diameter, so the M3 screw holes were drilled manually.

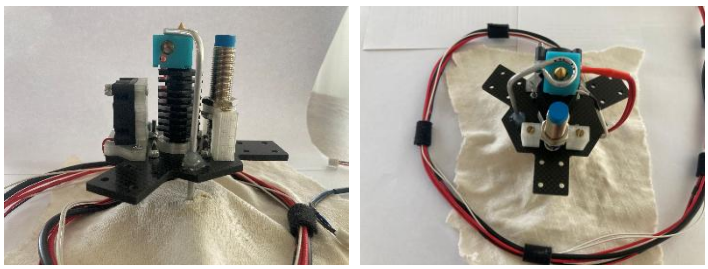

Fig. 5. End platform equipped with an extruder, a fan, and an inductive sensor

F. Extruder

The first part of the extruder consists of a small NEMA17 stepper motor, mounted at the bottom of the printer's base, combined with a 3:1 gearbox (BMG Dual Drive extruder). A standard Bowden tube guides the filament to the second part of the extruder, which is located on the end platform.

The second part of the extruder includes a coupling, which connects the Bowden tube from the stepper motor to a high-temperature Bowden tube. This tube passes through the heatsink and heatbreak all the way to the heatblock, ensuring precise filament retraction during printing. Additionally, the second part of the extruder consists of a 40 W heating element, an NTC 3950 100K thermistor, and a 0.4 mm brass nozzle.

IV. ELECTRONICS

Rotary delta 3D printers are not very widespread. However, when analyzed in detail, they are structurally very similar to linear delta printers. The same applies to their composition in terms of electronic components.

A. Endstop Detection

When analyzing the kinematics of this type of printer, despite the limited amount of literature on the subject, it is evident that a significant challenge lies in determining the endstop position of the arms. There are various methods for detecting end positions in 3D printers, such as mechanical switches, optical sensors, inductive sensors, and others. For accurate operation and coordinate recalculations, it is essential to determine as precisely as possible the angle formed by the printer's arms.

In the design of this printer, microswitches were chosen for endstop detection because they are inexpensive, fairly precise when positioned correctly, and easy to mount.

B. Control Electronics and Power Supply

The next step was selecting and integrating the electronic components of the printer. Due to the relatively simple composition of the components, a 24 V, 350 W power supply was used. This power supply is mounted on the printer's side using a 3D printed mounting bracket.

Also located under the base is a DIN rail with a quick terminal block, which distributes the power supply’s output voltage to other components. These components include: a 32-bit BIGTREETECH SKR V1.4 TURBO mainboard equipped with four TMC2209 stepper drivers, a Raspberry Pi (RPi) 4B with active cooling, a 24 V to 5 V buck converter for powering the Raspberry Pi, and a MOSFET module for PWM control of the air pump. Communication between the RPi and the mainboard is handled via a USB-B cable.

Additionally, the printer is equipped with a Mini 12864 RGB LCD display.

Printer is controlled by Klipper firmware using the Rotary_delta kinematics. It is operated via the Mainsail web interface [6].

V. PRINT TESTING

After thorough calibration of the printer, several test prints were conducted. First, a 15x15x15 mm cube with double walls

and 20 % infill was printed using a 0.4 mm nozzle and PLA filament. The print speed was set to 30 mm/s, the extruder temperature to 210 °C, and the bed temperature to 60 °C. Despite being printed upside down, the cube held well to the bed throughout the print.

Due to backlash in the arm and joint mechanisms, significant ghosting occurred on the printed object, and the cube tapered as it moved away from the bed.

Subsequently, several cylinders with a diameter of 15 mm and a height of 50 mm were printed using the same slicer settings as the mentioned cube. The print results for all three cylinders were similar to that of the cube, with slight variation. During printing, the cylinder's diameter alternately shrank and expanded. This could have been caused by the mentioned backlash in the used gearboxes and some faulty joints. The printed objects are shown in Figure 6.

By using a different type of gearing, high-quality spherical joints, and potential input shaping calibration, better results could be achieved.

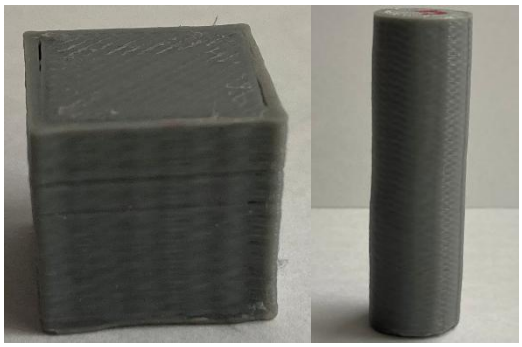

Fig. 6. Example of test prints

VI. CONCLUSION

The goal of this work was to design, assemble, and commission an FDM printer of the rotary delta type. Ultimately, the following objectives were achieved. All proposed main structural components were designed, manufactured, and assembled. By utilizing composite carbon materials, a low weight of the moving parts was achieved, which should improve both print quality and speed once the printer is fully operational and fine-tuned.

Additionally, thanks to the chosen joint type, an acceptable print area of approximately 220 mm in diameter was achieved. On the other hand, the resulting print volume height is limited to around 150 mm. Theoretically, with a small modification to the frame, it would be possible to increase the print bed diameter to approximately 260 mm at the cost of reducing the print height to around 110 mm.

Due to last-minute changes in the arm drive design, the described printer is currently unable to produce accurate prints. The main issue lies in the spherical joints and planetary gearboxes used to drive the arms, which exhibit excessive backlash in their current configuration. This results in print imperfections, as mentioned in chapter V.

Because of delays in the delivery of components and the ongoing tuning process aimed at minimizing mechanical imperfections, the printer is still in the final adjustment phase. However, after the installation of the new drive system and overall mechanical fine-tuning, the print quality is expected to improve significantly.

The final assembled design of the printer is shown in Figure 7.

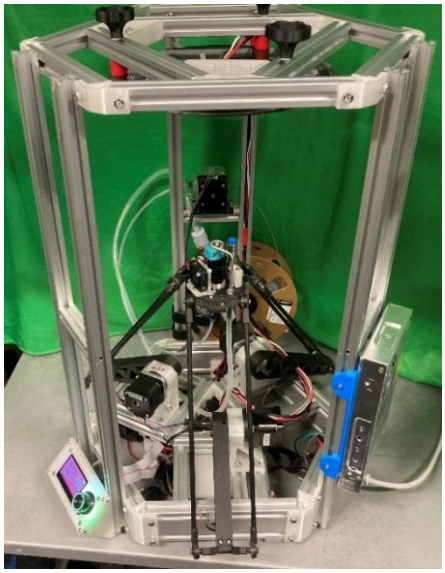

Fig. 7. The assembled printer is a rotary delta type

ACKNOWLEDGMENT

Thank you to my supervisor, Ing. Robert Bayer, for his help and advice during consultations and the preparation of my article.

REFERENCES

[1] Rotary Delta Printer. MyMiniFactory, Egris. Online. February 15, 2021 [cit.2025-02-24]. Available at: https://www.myminifactory.com/object/3d-print-rotary-delta-printer-154247

[2] Design of 3DOF Delta Parallel Capture Robot with High Speed and Light Weight. JUN-LIN, Ma; YING, Liu; YING-KUN, Zhang a CUNMING, Hao. Online. *Journal of Physics: Conference Series*. 2022, roč. 2188, č. 1. ISSN 1742-6588. [cit.2025-02-24] Available at: https://iopscience.iop.org/article/10.1088/1742-6596/2188/1/012008

[3] Workspace Analysis of Delta Robot Based on Forward Kinematics Solution. C. Liu, G. -H. Cao and Y. -Y. Qu. 2019 3rd International Conference on Robotics and Automation Sciences (ICRAS), Wuhan, China, 2019, pp. 1-5, doi: 10.1109/ICRAS.2019.8808987. Online. [cit. 2025-02-25]. Available at: https://ieeexplore.ieee.org/document/8808987

[4] Delta Robot: Working Advantages and Applications. Smlease Design. Online. [cit.2025-02-25]. Available at: https://www.smlease.com/entries/automation/delta-robot-working-advantages-applications/

[5] ŠABART, Adam. Paralelní kinematické struktury průmyslových robotů. Brno: University of Technology, Faculty of Mechanical Engineering, 2015. 52 pages. Bachelor's thesis supervisor doc. Ing. Radek Knoflíček, Dr. [cit.2025-01-03]. Available at: https://www.vut.cz/www_base/zav_prace_soubor_verejne.php?file_id=103516

[6] Klipper documentation. Klipper. Online. [cit.2025-03-09]. Available at: https://www.klipper3d.org/